Millimetro: mmWave Retro-Reflective Tags for Accurate, Long Range Localization

Elahe Soltanaghaei*
Carnegie Mellon University
esoltana@andrew.cmu.edu

Akarsh Prabhakara*
Carnegie Mellon University
aprabhak@andrew.cmu.edu

Artur Balanuta*
Carnegie Mellon University
artur@cmu.edu

Matthew Anderson
University
of California, Berkeley
mga@berkeley.edu

Jan M. Rabaey
University
of California, Berkeley
jan@eecs.berkeley.edu

Swarun Kumar
Carnegie Mellon University
swarun@cmu.edu

Anthony Rowe
Carnegie Mellon University
agr@ece.cmu.edu

ABSTRACT

This paper presents Millimetro, an ultra-low-power tag that can be localized at high accuracy over extended distances. We develop Millimetro in the context of autonomous driving to efficiently localize roadside infrastructure such as lane markers and road signs, even if obscured from view, where visual sensing fails. While RF-based localization offers a natural solution, current ultra-low-power localization systems struggle to operate accurately at extended ranges under strict latency requirements. Millimetro addresses this challenge by re-using existing automotive radars that operate at mmWave frequency where plentiful bandwidth is available to ensure high accuracy and low latency. We address the crucial free space path loss problem experienced by signals from the tag at mmWave bands by building upon Van Atta Arrays that retro-reflect incident energy back towards the transmitting radar with minimal loss and low power consumption. Our experimental results indoors and outdoors demonstrate a scalable system that operates at a desirable range (over 100 m), accuracy (centimeter-level), and ultra-low-power (< 3 uW).

KEYWORDS

millimeter wave,backscatter,localization, retro-reflective tag, FMCW, automotive radar

ACM Reference Format:
Elahe Soltanaghaei, Akarsh Prabhakara, Artur Balanuta, Matthew Anderson, Jan M. Rabaey, Swarun Kumar, and Anthony Rowe. 2021. Millimetro: mmWave Retro-Reflective Tags for Accurate, Long Range Localization. In *The 27th Annual International Conference on Mobile Computing and Networking (ACM MobiCom '21), October 25–29, 2021, New Orleans, LA, USA.* ACM, New York, NY, USA, 14 pages. https://doi.org/10.1145/3447993.3448627

1 INTRODUCTION

"Can we build an ultra-low-power tag that can be accurately localized at centimeter-scale over extended distances (e.g. over hundred meters)?". While such a tag could enable many applications, we focus specifically on autonomous driving where vehicles need to quickly and accurately localize digital lane markers, road signs and other roadside infrastructure over long distances. Even as today's autonomous driving technology relies primarily on both visual sensing systems (e.g. cameras, LIDARs) and visual road-side infrastructure, such systems are vulnerable to obstructions such as dirt or debris and weather events such as rain and fog. Wireless localization systems offer a natural alternative given their resilience to obstructions and inclement weather. Yet, current RF-based tag localization solutions strike a trade-off between device power consumption and range. Some solutions such as GPS, WiFi and UWB are high-power and would require frequent battery replacement of roadside infrastructure. Other solutions based on RF backscatter such as RFIDs are ultra-low-power yet limited in range to around 5-10 meters. While recent backscatter advances have sought to improve the range of these tags, they require frequency-hopping or measurements over extended time that are ill-suited to low latency requirements of the autonomous vehicle context.

Our design constraints of high-accuracy at low-latency naturally leads us to a solution that operates at the millimeter-wave (mmWave) frequency bands. mmWave bands offer large swaths of bandwidth that are contiguous and can be explored at a high data rate – i.e. no hopping needed, allowing for the system to operate at low latency. Further, we can re-use mmWave-based collision radars that are already a staple in cars globally, easing adoption by automotive OEMs. The core challenge, however, is that mmWave is notorious for its

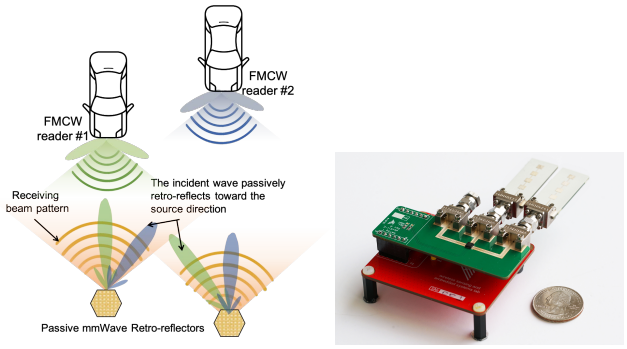

Figure 1: Millimetro is an ultra-low-power mmWave retro-reflector that supports accurate localization at long-range. Millimetro gets its long-range from reflecting back incident waves directionally towards the reader, and accuracy from the large bandwidth available at mmWave.

*Co-primary authors

ACM MobiCom '21, October 25–29, 2021, New Orleans, LA, USA
ACM ISBN 978-1-4503-8342-4/21/10.
https://doi.org/10.1145/3447993.3448627

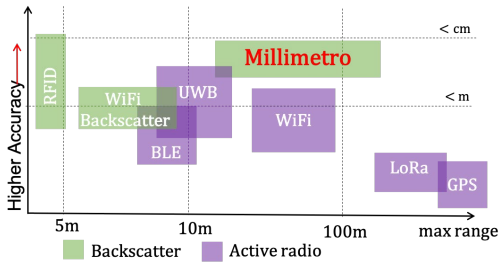

Figure 2: Millimetro significantly advances the range of current ultra-low-power backscatter localization solutions while ensuring high accuracy.

significant free-space path loss [41]. The current mmWave collision radars merely rely on large target radar cross section – i.e., a large surface area of the target (e.g. a vehicle-sized object) – to detect and localize targets at long ranges. However, the reflections from compact tags in the surroundings would be scarcely detected.

This paper presents Millimetro, a long-range backscatter tag design that can be accurately localized relative to mmWave automotive radars (shown in Figure 1). Millimetro's key innovation is the design of a mmWave retro-directive tag which pushes the localization range, despite the severe path loss of mmWave bands. In addition, the Millimetro tag design is ultra-low-power ($< 3\mu W$) and uses super resolution techniques at the reader to enable accurate localization. We show how despite operating at the mmWave frequencies, Millimetro achieves over 100 meters of range while delivering centimeter accurate ranging indoors and outdoors, with applications to autonomous driving, robotics and beyond. Figure 2 demonstrates how Millimetroexpands the state of the art localization in these 3 axes. As such, our design makes three key contributions:

Retro-directive tag design to mitigate SNR loss: We first address the twin challenges that emerge from operating at mmWave, that experiences much higher path loss compared to sub-GHz frequencies, while working with a small form-factor tag with a poor Radar Cross Section (RCS). Operating within the power budget of the transmitter, one naive solution would be to make the tags directive using large antenna arrays. However, this requires active phased array radios and constant beam steering for mobile scenarios. Instead, we keep the tag passive and achieve directivity using Van Atta arrays [49]. This approach is inspired from passive optical retro-reflectors embedded in road signs and lane markings which reflect light from the headlights back to the vehicle. Unlike optical, RF retro-reflectors allow operation in harsh environments, varying lighting and weather conditions. Van Atta arrays are completely passive and reflect any signal arriving in any direction, back toward their arrival direction. This retro-directivity provides the desired signal gain, tackles mobility and reduces interference while keeping the tag passive.

Asynchronous tag-reader operation: One of the challenges in contexts with mobility, such as autonomous vehicles, and large scale, such as industrial IoT, is the ability to quickly and effectively localize tags while a large number of radars are present. To address this, we use a fully asynchronous tag-reader architecture, unlike an RFID tag-reader architecture where a medium access protocol is used to deal with concurrent tags and readers. Our choice of retro-reflective Van Atta arrays on tags allows for each reader to simultaneously obtain a distinct reflection of its own transmitted signal, allowing for multiple radars to co-exist and locate tags without impact on latency. In effect, we piggy-back on the ability of the mmWave radars to detect and locate multiple targets simultaneously and avoid interference with other radars. Additionally, the tag circuitry remains simple in favor of an ultra-low power consumption.

Accurate tag identification and localization: While the fully asynchronous tag-reader architecture provides the desired low latency, it brings up new challenges on tag identification and localization as the radar has no notion of tag operation status during scanning. This is even more challenging in multipath-rich environments such as urban settings or cluttered industrial spaces, in which the received signal will be significantly dominated by static multipath reflections. To address this, we define a time-invariant modulation scheme on top of the Van Atta structure, and build on traditional radar processing techniques to detect the unique signature of the tags modulation and accurately localize them using a super-resolution technique. The tags coded modulation also avoids nearby tags interfering with one another. This allows for further scaling with number of tags and readers with minimal latency, as tags can communicate independently and simultaneously without coordination with either other tags or the readers.

Our system is built using off-the-shelf mmWave radars operating at 24 GHz with 250 MHz of bandwidth (conceptually our system applies to 77GHz radar as well). Millimetro is a custom designed backscatter tag at 24 GHz with several features such as Van Atta arrays and ultra-low power circuitry. We evaluate our system in indoor and outdoor settings and show that Millimetro achieves median accuracy of 15 centimeter in localization over distances of 100 meters. Millimetro incurs a power consumption of 2.36μW with continuous tag modulation at the frequency of 300 Hz, while running on a 3V CR2032 lithium coin cell which is comparable to the internal discharge rate of most batteries (25.6 years of life given CR2032 capacity) and can uniquely identify multiple uncoordinated tags from multiple uncoordinated readers in the same RF collision domain.

Contributions: Our core technical contributions are:

- Millimetro is the first system design of an ultra-low-power modulating mmWave retro-reflector that achieves centimeter-accuracy in ranging over distances of 100 meters.
- We present a novel low-latency asynchronous architecture to locate multiple tags from multiple readers.
- Millimetro is implemented and evaluated on commercial mmWave automotive radars and is demonstrated in proof-of-concept deployments indoors and outdoors.

2 DESIGN SPACE

In this section, we first define our motivation for a retro-reflective solution to address the power vs. range trade-off in backscatter localization. We then explain how its combination with mmWave technology ensures high localization accuracy while retaining long range, achieving the best of both worlds.

2.1 Why Van Atta Retro-directive Tags?

In radio transmission, phased arrays and smart antennas have been one of the conventional methods for increasing received signal power and accordingly the operating range of wireless systems by creating directional transmissions. However, the high power consumption and

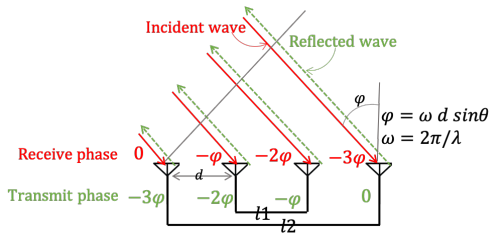

Figure 3: The Van Atta retro-directive array is a passive design that reflects back any incident wave in reverse, parallel to the direction of incidence.

complexity of beam steering and beamforming systems disqualify such solutions in the design of low power tags.

This leads us to retrodirectivity, the capability that solely uses analog RF components to reflect an incident signal towards the source direction without any prior knowledge of its direction of arrival. The concept of retrodirectivity comes from corner reflectors, that were originally proposed for long-range radar applications such as lunar laser ranging by installing such a device on the moon [4]. Corner reflectors use orthogonal metal sheets [13] to reflect incoming radio waves back along the exact same direction as the incoming waves. However, these passive reflectors have limited functionality and are bulky. With the development of high-frequency electronics, RF retro-reflectors have become more accessible by providing capabilities such as signal modulation. There are two methods to achieve retrodirectivity in wireless systems: phase conjugate arrays and Van Atta arrays.

Phase conjugate arrays: These arrays use heterodyne techniques [39] to conjugate the phase of incoming signal at each antenna element by mixing it with a local oscillator (LO). This results in a radiated beam back toward the source direction. However, such design requires a mixer circuit with a large frequency difference between RF and LO signals, which makes the array complicated, bulky and power hungry – and therefore unsuitable for our purposes.

Van Atta array: Van Atta array is another method for achieving retrodirectivity, which first appeared in 1959 [49]. As illustrated in Figure 3, they consist of an array of antennas that are connected in symmetrical pairs by transmission lines of equal length or length differences equal to multiples of the guided wavelength – i.e. the transmission lines do not contribute additional phase difference to incident waves. Every antenna in this array serves as both receiving and transmitting antennas. The signal received by each antenna is transmitted through the line and re-radiates from the corresponding paired antennas. Observe in Figure 3 that every antenna and its pair are arranged in a mirror symmetric manner – i.e. the first antenna is connected to the last, the second to the penultimate, etc. This arrangement of the array and feed network is deliberate – it causes a relative phase reversal for the reflected wave when compared to the incident wave. The result is that all energy incident to a Van Atta Array is simply reflected back along the precise direction of incidence. Unlike phase-conjugated arrays that require active components, Van Atta arrays can be designed completely using passive components, which makes it well-suited for low-power backscatter.

A brief mathematical primer on Van Atta arrays: To understand the retro-directivity of passive Van Atta arrays, let us consider an N-element array as shown in Fig. 3. Consider a signal received at an angle θ, a relative phase shift of $[0,-\varphi,-2\varphi,..,-(N-1)\varphi]$ across the antennas are expected, where $\varphi = 2\pi d \sin\theta/\lambda_g$, and d is inter-element spacing and λ_g is the guided wavelength of the signal. The received signal by m^{th} antenna ($m=1,...,M$) travels through a transmission line of length l_m, to re-radiate out from the corresponding paired antenna $(N-m+1)$, resulting an extra phase shift of $2\pi l_m/\lambda_g$ (see Fig. 3). Since the connecting transmission lines in between are designed to have equal lengths l_m (or differ by multiples of wavelengths), the phase shifts due to all these lines are effectively equal. As a result, we can see that the signals radiating out from the array will have a reversed phase distribution of $[-(N-1)\varphi,-(N-2)\varphi,..,-2\varphi,-1\varphi,0]$ compared to the incident signals. We leverage this property of Van Atta arrays to increase the received signal strength by ensuring that it is focused specifically along the direction of the reader, thus increasing the operating range of backscatter systems. We later elaborate on how modulation can be added to the Van Atta structure while preserving ultra-low-power consumption.

2.2 Why mmWave Backscattering?

Accurate ranging and therefore localization, requires high bandwidth for high temporal resolution. However, wide ISM bands are not available in lower frequencies. Recent work tried to address this problem by using channel stitching and frequency hopping techniques [33, 36] to emulate a wider bandwidth at the expense of hopping latency. However, a more apt long-term solution to this problem is to leverage the large, contiguous multi-GHz unlicensed bandwidth in mmWave frequency bands. More importantly, the short wavelength of the signal in these frequencies enables the implementation of large antenna arrays in a small form-factor. This can significantly improve the performance of Van Atta retrodirective arrays as it allows to improve the signal SNR and radar cross section of the backscatter device without losing the angular aperture as apposed to conventional antenna arrays. As such, the combination of Van Atta arrays and mmWave operating frequency enables long range and low power (properties of Van Atta) as well as accurate localization and compact form factor (properties of mmWave) – bringing together the best of both systems.

While free-space path-loss for mmWave frequency bands is higher when compared to lower frequencies (a problem we address through retro-directivity), it should be noted that they do benefit from stronger reflections from tags in the backscatter context that mitigates our challenge to some extent. To see why, note that, backscatter systems mainly rely on switching the input impedance at the tag to create two states and modulate the backscatter signal. At each impedance state, the tag presents a certain radar cross section (RCS) and maximizing the differential RCS of the two states allows greater ease in tag detection and identification. Based on the theory of loaded antenna RCS [13], the radar cross section of a backscatter tag, expressed as $\sigma = \frac{4\pi e_t^2 A_t^2}{\lambda^2 |\Gamma_{A,B}|^2}$, is inversely proportional to the wavelength. $\Gamma_{A,B}$ is the reflection coefficient of the two states, e_t is the aperture efficiency of the tag antenna and A_t is the physical area of the tag. For a fixed effective aperture, higher frequency operation offers significant gain in backscatter signal detectability.

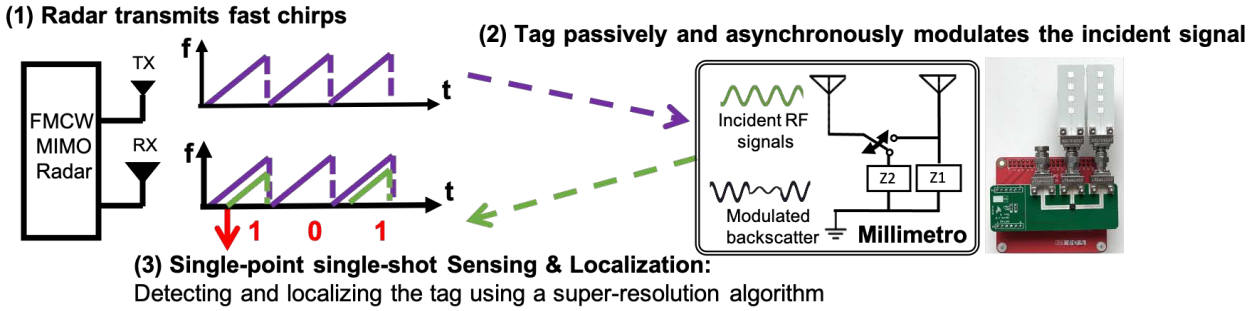

Figure 4: System Overview

3 SYSTEM OVERVIEW

We present *Millimetro*, a novel backscatter localization system, which uses mmWave retro-reflectors and frequency modulated continuous-wave (FMCW) radars to enable *long range and accurate* backscatter localization. An overview of the Millimetro localization system is depicted in Figure 4. The tags continuously modulate and retro-reflect any incident signal, which are then identified and localized by an FMCW MIMO radar. The radar transmits fast chirp signals (in the order of μs), each occupying the entire ISM band available in mmWave frequency range (e.g. 250 MHz bandwidth in 24 GHz). It then receives the echo of the transmitted signal and analyzes that locally to identify and localize the tag.

Millimetro's tag-reader architecture: The conventional backscatter communication systems such as RFID use a handshake protocol between the tag and reader to interrogate the tag and wakes it up for responding to the reader. However, such protocol relies on time-multiplexing in a multi-tag multi-reader scenario, resulting in significant added latency. In addition, in a dynamic setup such as autonomous driving, it is more challenging for the readers to coordinate with each other in a timely manner. Here, we leverage the retro-directivity as an opportunity for an alternative tag-reader architecture. In this design, we make the energy source of the tag independent from the backscatter localization system. The tags are continuously modulating any incident signals independent from the reader operation. This greatly simplifies the tag circuitry by not requiring any computational logic, envelop detector or decoding components, making it low power and suitable for scale deployment. In addition, thanks to the retro-directivity properties, the tag can simultaneously respond to multiple readers by minimizing potential interference, resulting in a *concurrent multi-tag multi-reader* operation. However, the continuous operation of the tag, presents new challenges on the tag design to achieve ultra-low-power consumption. Section 4.2 elaborates on Millimetro's ultra-low-power modulation scheme.

In summary, Millimetro consists of two main components to satisfy the aforementioned desired features (low power, long range, and accurate localization):

- **Ultra-low power retro-directive tags:** Millimetro leverages Van Atta arrays to increase the operating range of the tag without requiring complex and high power components. Combined with short wavelength of mmWave signals, Millimetro tags are equipped with large, but compact Van Atta arrays to further improve the backscatter retrodirectivity without reducing the angular aperture. However, the significant path loss of mmWave signals can result in high in-band interference in multipath-rich environments. Section 4 explains how Millimetro leverages retro-reflective modulation to increase the differential radar cross section of the backscatter signal, thus improving the tag detectability.
- **Single-source super-resolution tag localization:** Millimetro leverages commercial FMCW MIMO radars to provide single point localization by estimating the range and angular properties of the retro-reflected signal. Millimetro radar identifies the tags by searching for the unique signature of Van Atta modulations in the range-Doppler domain. However, the range and angular resolutions are still limited by chirp bandwidth and the number of receiving antennas. Section 5 discusses Millimetro super-resolution techniques to fine-tune the range and angular estimates of the tag retro-reflection and perform localization.

4 MILLIMETRO TAG ARCHITECTURE

4.1 Retro-directive Van Atta Design

As shown in Figure 1, the simplest version of the Millimetro tag consists of a pair of antennas connected to each other with a transmission line. An RF switch is placed within the line to modulate the retro-reflected signal by either guiding the signal to the paired antenna creating retro-reflection, or to a load to break retrodirectivity. While this is the most compact and simple version of a Millimetro tag, more elaborate multi-antenna designs can trade-off additional space to improve radar cross-section and therefore range.

Our design of Millimetro therefore builds on a linear Van Atta structure with each element of the array as a 4-element linear series-fed patch array for extra gain (see Figure 5). This allows us to keep a large beamwidth along the plane of retrodirectivity while compensating the beamwidth in the orthogonal plane to increase the overall antenna gain. In addition, the series fed patch array elements with high gain allows maximization of RCS with the minimum number of components for modulation. The patches on every Van Atta element are followed by a quarter wave transformer to provide high S11 characteristics.

The transmission lines in the Van Atta array are another important factor affecting the retro-directivity performance. The induced phase delays of each feedline network relative to other lines (from 1 to N, relative to 2 to $N-1$,etc) should be identical. This is theoretically possible by choosing the line length proportional to the wavelength. However, it becomes more challenging when inserting a switch in the middle of each transmission line. To address this requirement, we break each line into two parts, from each antenna to the switch and tune the length of each line segment such that the phase shift across

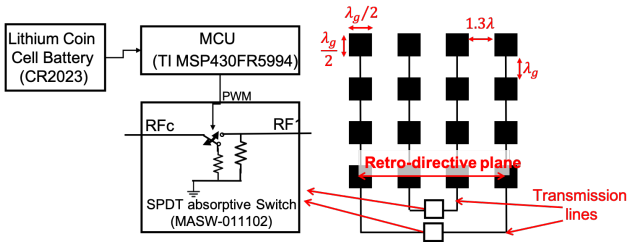

Figure 5: Millimetro tag uses a Van Atta array structure modulated by RF switch controlled by a low power microcontroller running on a coin cell battery.

corresponding parts of antenna pairs encounter similar phase shifts in the center frequency (shown in Figure 10b).

4.2 Modulation of the Retro-reflected Signal

Backscatter modulation is one of the conventional ways for tag identification and coding gain, which is usually obtained by either using amplitude, phase, or frequency modulation. The fully asynchronous tag-reader architecture has both positive and negative impacts on power consumption. On one hand, this makes the tag free of any computational logic or power hungry components such as phase-shifter, envelope detector, decoder, or high frequency oscillator. However on the other hand, this asynchronous operation necessitates the tag to continuously perform modulation for any incident signal at any time, resulting in higher power consumption. To optimize this trade-off, we select a power-efficient modulation scheme that allows the tag to continuously run the modulation while consuming as low as $2.36\mu W$ with a scanning and localization latency of $38ms$.

Among the potential modulation schemes, the conventional on-off keying best suited for the Van Atta structure as it can be simply obtained by a passive ultra-low-power RF switch inserted within each Van Atta transmission line. When the switch is in the on-state, the incident waves go through the transmission lines resulting in high returning field toward the direction of the signal. When the switch is in the off-state, both the antennas get terminated by a matched load, destroying the retrodirectivity by generating near zero return signal. This maximizes the on-to-off RCS, resulting in higher detectability. We select GaAs absorptive Single Pole Double Throw (SPDT) RF switches as apposed to Pin diodes for their lower power consumption. In addition, the non-reflective configuration of the switch allows simultaneous load matching of both antennas in the off-state. The next section elaborates on how Millimetro identifies the tag modulation in the absence of any time synchronization between the tag and the radar.

5 MILLIMETRO AT THE RADAR

Millimetro leverages commercial FMCW MIMO radars to identify and locate tags. During the operation, the radar transmits multiple chirps each occupying the entire available bandwidth. In the presence of an active tag in the field of view of the radar, the incident signal at the tag gets modulated and retro-reflects toward the radar. The radar receives this signal at its antenna array and multiplies it by the transmitted signal, creating a difference *intermediate frequency (IF)* signal. The IF signal is then analyzed to identify the tag retro-reflection and extract the corresponding range and azimuth information.

One of the main challenges in detecting the tag is the asynchronous functionality of the tag and the reader. The radar has no notion of when the tag started the modulation and it is very well possible that the tag toggles in the middle of a chirp resulting in a corrupted reflected signal. In addition, in multipath-rich environments, the radar has to deal with large dynamic ranges due to other reflections in the environment such as second-order reflections from the radar to the tag and vice versa. Millimetro exploits state-of-the-art signal processing solutions to address this challenge. In the next section, we first explain how Millimetro exploits the unique properties of on-off keying modulation in the frequency domain to identify the tag and then elaborate on Millimetro's localization algorithm.

5.1 Tag Identification

After downchirping the received signal at the radar and analog-to-digital conversation at the sampling frequency f_s, the IF output signal can be modeled as

$$s_{IF}(n) = \alpha \sin(\frac{4\pi B}{Nc_0} rn) \tag{1}$$

where α is the amplitude of the signal, N is the number of samples taken, c_0 is the speed of light, and r is the distance to the target. In the presence of an active tag attached to the target, the on-off keying appears as a square wave with the switching frequency of $f_{switch} = 1/T_{switch}$.

$$s_{IF}(n) = \alpha \sin(\frac{4\pi B}{Nc_0} rn) \cdot \sum_{k=-\infty}^{\infty} rect(\frac{2(nT_s - kT_{switch} - t_0)}{T_{switch}}) \tag{2}$$

where t_0 denotes a random time shift as the FMCW chip and the tag switching are not synchronous and is unknown to the radar due to asynchronous operation of the tag and the reader. To address this problem, Millimetro performs the tag detection and localization in the frequency domain to create a time-invariant signature of tag modulation. During the operation, Millimetro radar triggers N_c fast chirps within a frame and records the IF signals. Then, it uses the received signal for the first chirp as the reference for background subtraction. This allows to eliminate dominant multipath reflections from surrounding objects such as the road sign itself or nearby cars in the autonomous application. It should be noted that the tag identification only relies on the differencial RCS due to tag modulation which will be preserved even after background subtraction. Finally, we perform a 2-dimensional Fourier transform for each chirp inside a frame to estimate the *range-FFT* map of the channel. Therefore, the modulated tag signal appears in the FFT output at the tag's corresponding range bin. A snapshot of FFT output can be seen in Figure 6 at the 7 m range bin, where the tag was located.

However, the random time shift still exist across chirps due to asynchronous operation of the tag and reader. To eliminate this offset, we perform another FFT operation called *range-Doppler*, which converts the square wave across chirps to a sinc function with the primary frequency component equal to the modulation frequency. The unique signature of the tag modulation in the range-Doppler map also allows us to differentiate the tag reflection from other dynamic reflections. As such, Millimetro identifies the tag retro-reflection and the corresponding range bin by match filtering the expected sinc template $P_A(f_{switch})$ across range bins:

$$P_A(f_{switch}) = FFT(square(2\pi T_s f_{switch})) \tag{3}$$

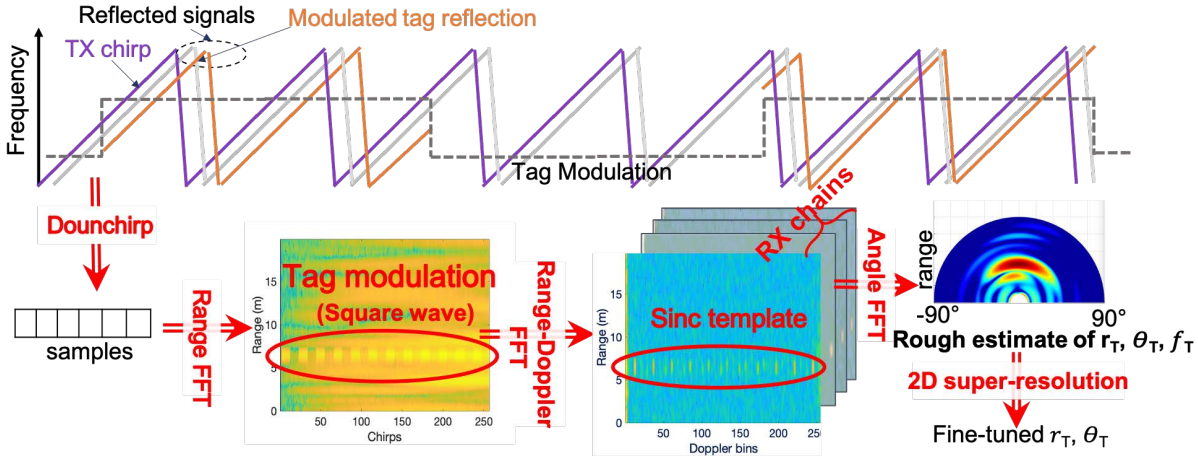

Figure 6: Millimetro Reader analyzes a series of FMCW chirps, searches for tag modulation using template matching, identifies the tag and then localizes it using a combination of FFT and MUSIC algorithms.

where f_{switch} is the tag's modulation frequency, square(.) is a periodic square function, and T_s are the chirp sampling time corresponding to radar's chirp repetition frequency. However, in a multipath-rich environment, the radar may receive more than one copy of the retro-reflected tag signal (i.e. a second order reflection that reached to the tag from a strong reflector in the environment) and the match filtering may result in a higher correlation for the multipath signal than the direct path between the tag and the reader. To avoid such confusions, Millimetro defines a threshold and selects the shortest range bin that passes the correlation threshold. It should be noted that the threshold defines a trade-off between localization accuracy and false alarms, which is studied in the evaluation section.

Similarly, the tag can be identified in the azimuth plane by using the phase difference between receiving antennas. Millimetro performs the range-Doppler processing for all the receiving antennas. Each peak of the Doppler-FFT contains phase information for every reflection including the Millimetro tag. Therefore, a discrete FFT over the sequence of antennas results a *range-angle* map with peaks at the corresponding tag locations (shown in Figure 6).

Mobility: In mobile scenarios where either the tag or the radar is moving, the tag's modulation frequency will be shifted by the Doppler frequency corresponding to the relative velocity of the tag and radar. Therefore, the received signal from the tag appears as

$$s_{IF}(n) = \alpha \sin\left(\frac{4\pi B}{Nc_0}(r + vT_c)n\right) \cdot \sum_{k=-\infty}^{\infty} rect\left(\frac{2(nT_s - kT_{switch} - t_0)}{T_{switch}}\right) \tag{4}$$

where v is the relative Doppler velocity and T_c is the chirp duration. Therefore, Millimetro can be simply extended to mobile scenarios by refining the match filtering template to account for expected Doppler velocity as

$$P_A(f_{switch}, v) = FFT[rect(2\pi T_s f_{switch}) \cdot cos(2\pi(2vf_c/c_0)T_c T_s)] \tag{5}$$

where f_c is the center frequency of the transmitted signals. Millimetro defines a 2D template matrix for the corresponding tag modulation frequencies and expected Doppler velocities and selects the (f_{switch}, v) tuple with the highest correlation across range bins of the range-Doppler map. It should be noted that the presence of other moving objects such as surrounding cars does not affect the match filtering process as Millimetro relies on the direct retro-reflection from the tag to the radar. However, such dynamic paths may result in ambiguity as the Doppler frequency of these reflections also appear in the second FFT. Millimetro avoids such ambiguity by (1) defining the modulation frequencies far enough from the Doppler frequency range of moving cars, (2) defining the match filter based on the sinc template rather than the primary frequency component. The intuition is that the Doppler shift due to moving surrounding objects is a single frequency component in the range-Doppler map, while the tag on-off keying appears as a sinc function with harmonics in known frequencies.

Modulation Rate vs. Chirp Duration vs. Power: Note that the tag modulation rate is a function of radar's chirp duration and the tag's power budget. On one hand, Millimetro at least needs to receive a full modulation period without in-chirp corruption to detect the tag. On the other hand, the modulation rate should be proportional to the available power budget at the tag (either using a battery or harvesting energy). Therefore, we define the tag modulation frequency as $f_t = \frac{1}{2*(kT_c)}$, where T_c is the radar chirp duration and k is a constant scalar. In the worst case scenario, every tag switching may result in a corrupted chirp, then by selecting $k > 3$, Millimetro can guarantee the reception of at least one full tag modulation in each frame. In this paper, we define T_c in the order of $150-350us$ and the tag modulation period in the order of $3-10ms$.

5.2 Single-source Tag Localization

To locate the tags in the physical space, the tag range estimate can be combined with the angular properties of the retro-reflection by leveraging the antenna array at the radar. The combination of range and angles allows Millimetro to locate the tags locally from a single vantage point without requiring any sort of triangulation or trilateration. Combined with the small form factor of mmWave MIMO radars, this enables Millimetro to be used as a portable backscatter localization system in a variety of applications such as urban sensing, industrial IoT, or augmented reality.

While the tag identification module, explained in the previous section, provides a rough estimate of the tag's distance and azimuth to the

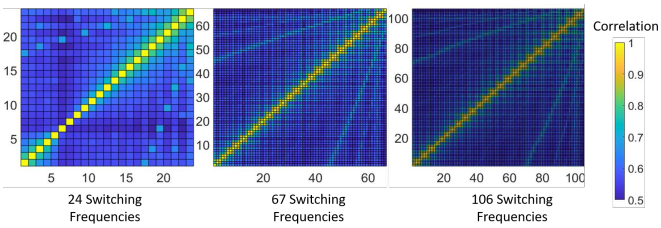

Figure 7: Gram Matrix characterizing the degree of correlation between sinc template functions corresponding to different switching frequencies.

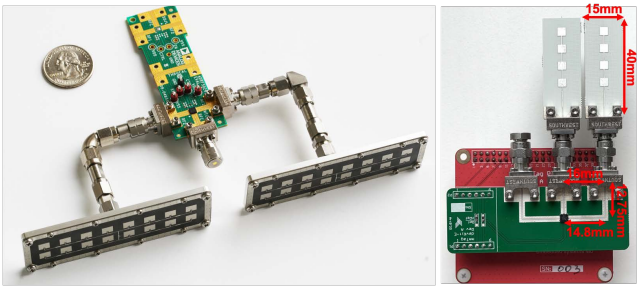

(a) Prototype assembled using off-the-shelf components (b) Integrated PCB prototype

Figure 8: Millimetro Tag Prototypes

radar, the resolution of FFT-based estimates are limited in multipath-rich environments. On the other hand, super-resolution techniques such as MUSIC [53] provide higher resolution at the expense of high computational overhead. To address this issue, we use the rough estimates from the identification process as the initial estimate of tag's range and azimuth angle to limit the search space and refine these estimates by using a super-resolution algorithm. The sampled signal within a chirp can be written as

$$s(n) = \sum_{p=1}^{P} \gamma_p \cos(2\pi S \tau_p \frac{n}{f_s}), n = 0...N-1 \quad (6)$$

where N is the total number of samples in a chirp, $S = B/T_c$ is the slope of each chirp B is the chirp bandwidth, and γ_p and τ_p are the complex amplitude and the time delay of target p. When the signal is collected by an array of antenna elements, a spatial sampling is also observed resulting on a new component in the time delay expressed as

$$\tau_p = \frac{2}{c}(r_p + ld\sin\theta_p), l = 0...L-1 \quad (7)$$

where r_k and θ_k are the range and azimuth of target p, c is the speed of light, d is the inter-antenna array spacing, and L is the number of receiving antennas. Therefore, a 2D MUSIC [53] algorithm can be defined for joint range-azimuth fine-tuning. The initial FFT-based estimates of the tag's range and azimuth angle also allows to limit the search space to the tag location and avoid spurious multipath estimates. Finally, the range and angular estimates can be used to directly localize the tag in the 2D physical space. In the presence of antenna arrays in the elevation plane of the radar, this formulation can be extended to a 3D joint-estimation of range, azimuth and elevation.

5.3 Concurrent Operation

Millimetro's asynchronous architecture both supports multiple tags and readers without compromising on read latency – important for the automotive context.

Multiple Tags: Millimetro's detection and localization algorithm is designed such that it can separate multiple active tags with different modulation frequencies. The intuition is that different modulation rates appear as sinc function with different frequency components in the range-Doppler profile. In other words, switching at a frequency f_t will result in peaks in the sinc function at $2\pi T_c f_t$, $2\pi T_c 3 f_t$, $2\pi T_c 5 f_t$, etc. To avoid collision, two different switching frequencies must peak at bins that are an integer away, that is $2\pi T_c \Delta f_t > \frac{2\pi}{N}$. This condition is sufficient to ensure that none of the peaks collide with peacks of other switching frequencies. For $N_c = 256$, upto 24 switching frequencies can be assigned such that no peak collides. For denser deployments, we relax the criteria to allow the first peak ($2\pi T_c f_t$) to collide, and ensure that subsequent peaks ($2\pi T_c 3 f_t$, $2\pi T_c 5 f_t$) don't collide. This changes the criteria to $2\pi T_c \Delta f_t > \frac{2\pi}{3N}$, thereby allowing more switching frequencies. This way we can relax the criteria as more and more tags are deployed. For $N_c = 256$, relaxing first peak collision gives us 67 frequencies and relaxing second peak collisions gives us 106 frequencies. Figure 7 shows the Gram Matrix, essentially cross correlation between different sinc templates after choosing switching frequencies according to our criteria. As designed, we observe that there is high autocorrelation and low cross correlation. Note that the number of tags choosing unique switching frequencies is required only if they are deployed in the same vicinity. Tags far away from each other can still have identical switching frequencies. We assume the modulation frequency of tags are select at the deployment time based on the number of tags that are present in each zone.

Multiple Readers: The retrodirectivity feature of the Millimetro's tags allows multiple radars to simultaneously localize a tag with no interference. Closely spaced radars (defined by the number of elements in the Van Atta structure) can still experience some interference. However, the combination of asynchronous operation of radars as well as the chirp structure of the transmitted signal significantly reduces the probability of two radars sending the same frequency at the same time. We evaluate the localization performance in the presence of multiple active radars in Section 7.5.

6 IMPLEMENTATION

We implemented Millimetro using a commercial mmWave MIMO radar, Analog Devices TinyRad[2], operating at 24 GHz with 250 MHz of bandwidth and maximum power output of 8 dBm. The radar integrates 4 on-board receiving antennas and 2 transmitting antennas. In this implementation, we only used one of the transmitting radio chains, sending the FMCW chirp over the full 250 MHz of bandwidth, and sampling the received signal at Rx1-Rx4. This configuration only provides 2D localization, however, Millimetro can be easily extended to 3D by the use of a 2D MIMO radar. In addition, Millimetro's architecture is independent of the operating frequency and can be extended to 77 GHz where larger bandwidth is available. The received signal is sampled at 1 MHz and captured using MATLAB, directly polling data from the board.

6.1 Millimetro Tag Prototyping

We developed multiple prototypes of the retro-reflective tag, as shown in Figure 8. Our first design uses ADRF5027 [1] RF switch evaluation

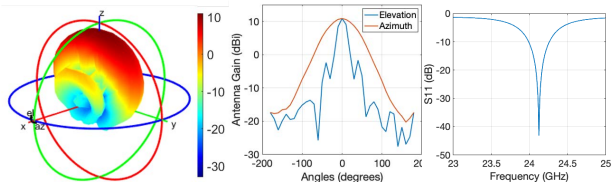

(a) Antenna Beam Pattern (b) S11 Parameters

Figure 9: Millimetro Antenna Prototype

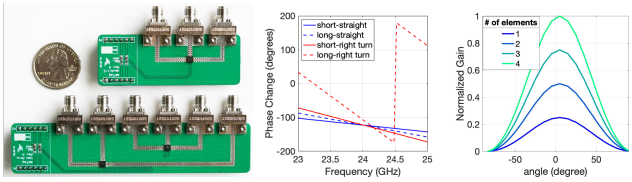

(a) Van Atta Prototypes (b) Phase (c) Van Atta gain

Figure 10: Van Atta Microbenchmark

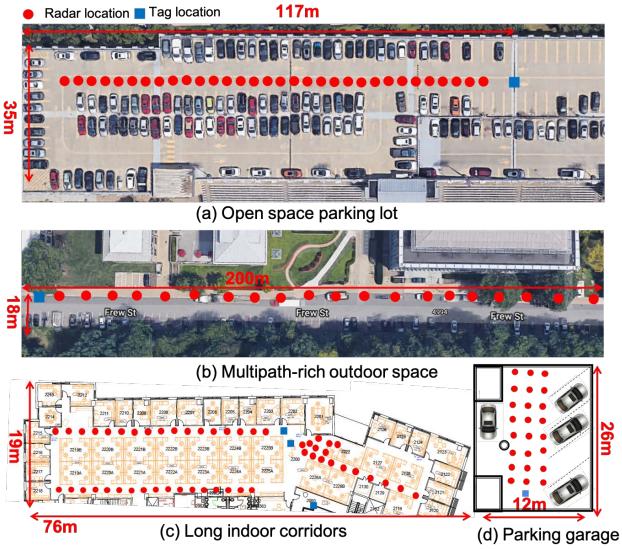

Figure 11: Experiments were conducted in four environments with different multipath complexity and ranges.

kit powered by an ATmega328P microcontroller and 2 off-the-shelf microstrip patch antennas each in a 2×8 array. The antennas are connected to RFC and RF1 ports of the switch, creating a 2-element Van Atta array, while RF2 is terminated with a 50Ω cap for on-off keying modulation. We use this prototype for all evaluations in Section 7.

The next prototype is optimized for power efficiency. As shown in Figure 8, it consists of a GaAs SPDT RF switch from MACOM [5] atop a Rogers RO4350B substrate that interconnects custom designed antennas (Figure 9 and 10) using Grounded CoPlanar Waveguides (GCPW) and 2.92 connectors. A Texas Instruments MSP430FR5994 microcontroller is used to control the RF switches. We have two versions of this board (see Figure 10a) - one specifically for a 2 element Van Atta array, and another modular design which allows varying sizes of arrays from 1 to 4 elements. Fully integrated versions of the Millimetro tag can be designed to be slightly bigger than a credit card. Note that the location of the switches within the feed lines is not important due to 50Ω termination of both antennas at the off-state. We select to position the switch at the corner of the transmission line to minimize wide angle turns along the transmission lines.

To achieve the desired retro-directivity discussed in Section 4.1, we match phases of the corresponding transmission line segments across the antenna pairs. Figure 10b demonstrates the identical phase at 24.125 GHz using one port reflection coefficient measurements. In addition, Figure 10c shows the expected re-radiated field [13] for different sizes of Van Atta arrays. As expected, the retro-directive gain increases for larger number of elements proportional to the beam pattern defined by the antenna. In Van Atta structures with more than one RF switch, special attention should be given to the RF switch control traces in order to ensure simultaneous activation. As shown in Figure 10a we make use of length controlled differential pairs to interconnect our microcontroller and RF switch to ensure the same propagation delay. Designs with 4 or more antenna element pairs will benefit from following a star distribution of the control signals as well as the same trace length.

6.2 Power Consumption

One of our key design challenges was to minimize tag energy consumption. Many high frequency RF switches draw a significant amount of power to maintain linearity, but the MACOM RF switch [5] works across our frequency band with a typical power consumption of less than $1\mu A$. We pair this with a MSP430FR5994 microcontroller [7] that operates across the entire battery voltage range and hence requires no voltage regulator. A single Timer domain is used to generate a PWM signal and control two output pins by using both edges of the PWM signal. By using the specialized timer subsystem, the microcontroller remains in a low-power sleep mode (LPM4) with an internal low-power low-frequency oscillator running and the RF switch maintaining its on or off state. Periodically, the timer subsystem will fire and automatically change the state of the RF switch. The entire process of changing the state of the RF switch and depleting the internal capacitance of pins and traces takes about $500ns$. Thus, the overall power consumption of the tag is dependent on the number of switch state changes. For a rate of 300, 600, 700, 900, 1100 state changes per sec, we measured an averaged power consumption of 2.36, 2.53, 2.61, 2.71 and $2.86\mu W$, using Keysight N6784A Source Measurement Unit (SMU). If paired with a small form factor $3V$ CR2032 lithium coin cell ($235mAh$) we predict that this tag could offer continuous operation for 20.1 to 25.6 years, assuming an efficiency of 75% and no battery self discharge. Certainly, this kind of batteries recommend a shelf life of about 10 years after which their performance is not guaranteed by the manufacturer [3]. Alternatively, this amount of power can easily be supplied by a number of energy harvesting or even atomic sources [6].

7 EVALUATION

We deploy our system in four different environments: (1) an open space parking lot with no cars, (2) a multipath-rich street (3) a roofed parking garage with multiple cars around the tag and radar, (4) an indoor office environment with long corridors, metallic chests, and a lot

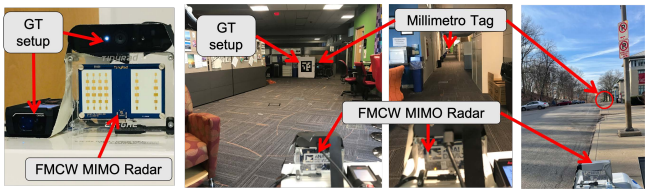

Figure 12: Snapshots of the experimental setup.

of furniture near both the tag and the radar, representing a multipath-rich indoor environment. The location of the tag and over 150 radar locations are depicted in Figure 11, with the snapshots of the tag and radar setups in Figure 12.

For the indoor experiments, we set the chirp time duration to 150 us with 256 chirps per frame. This results in a maximum detectable range of 37 m (at a radar with real data). For outdoor experiments, we increased the chirp time duration to 1ms with 64 chirps per frame to guarantee a maximum detectable range of 300 m. In each experiment 100 frames are collected per test location. For most of these experiments, if not mentioned specifically, we used the 2 element Van Atta structure with a 2×8 patched antenna array at each element.

Baseline: Our baseline is an otherwise identical backscatter tag with a regular scattering antenna as opposed to retro-directive antenna arrays. We isolate other factors by using the same localization and detection algorithm on both systems. We were unable to compare Millimetro's performance with the similar mmWave tags proposed in the literature, due to the limited public design details available and the high engineering effort involved in reproducing them correctly. It should be noted that the main difference of Millimetro's tag with similar mmWave tags is the ultra-low power consumption, which is comparable using the nominal values provided in Section 6.2.

Ground Truth: To collect the ground truth in shorter ranges (up to 40 m), we use a $60\times60cm$ Aruco marker and a camera installed on top of the radar, shown in Figure 11. At extended distances beyond 40 m where the marker does not operate, we used a combination of laser range finder and floor tiles.

7.1 Localization Performance

We evaluate the localization accuracy across all the experiments both in multipath-rich indoor and open outdoor spaces. Since the distribution of errors in range and azimuth estimates are different across extended ranges, we start with the performance of Millimetro in estimating each of these two parameters separately. As shown in Figure 13a, the median range error is 15 cm in both indoor and outdoor setups with a 90^{th} percentile of 60 cm. The main difference between indoor and outdoor experiments is at the upper 10^{th} percentile, where results show a longer tail for the indoor experiments. This is mainly caused by multipath propagation, especially in narrow corridors.

Figure 13b presents the azimuth estimation errors. By leveraging the radar's receiving antenna array , Millimetro achieves a median accuracy of 3 degree and a 90^{th} percentile accuracy of 10 degree across both indoor and outdoor experiments. Compared to the nominal azimuth resolution of the commercial radars (approximately 20 degree [2]), Millimetro's super resolution algorithm already enhances the accuracy of the angle estimates to a significant extent. However, given the extended operating range of Millimetro, the azimuth error estimates could have significantly different impact on 2D localization error across different ranges. For example, 2 degrees of azimuth error for a target at ranges of 5, 10, 20, or 100 m results in a 2D localization error of 0.17, 0.35, 0.7, 3.5m, respectively. However, considering the radar's mobility and the low latency of Millimetro in localization, aggregated tag readings over time as well as the Kalman filter techniques can be used to improve the localization accuracy. In addition, in many applications including autonomous driving, robotics, or industrial indoors, the azimuth accuracy over extended ranges is less important compared to shorter rangers. It should be noted that the number of radar's receiving antennas is one of the main factors defining the angular resolution. Therefore, this resolution can be further improved by simply using radars with larger arrays specially in mmWave frequency bands with the small form factor of antennas.

Nevertheless, for completeness, we also provide the 2D localization accuracy in both outdoor and indoor experiments in Figure 13c, which shows a median accuracy of 22 cm in open space outdoor experiments and 56 cm in multipath-rich indoor spaces. The long tails in this graph are the effect of azimuth errors in longer ranges as discussed earlier.

7.2 Operating Range

Next, we evaluate Millimetro's performance as a function of distance. To better understand the impact of Millimetro's retrodirectivity on extending the operating range, we compare it with a baseline method which uses a single antenna instead of a Van Atta structure. We repeat the experiments at open space outdoors and an office space indoors for the baseline at similar test locations shown in Figure 11. For a fair comparison, we keep all the other parameters the same between these two approaches including the modulation scheme and the localization algorithm. Figure 14a shows the detection rate of Millimetro compared to this baseline across different distances. We can see that Millimetro maintains an above 90% detection rate up to 100m and it gradually degrades to less than 20% at ranges over 200m. This is while the baseline approach significantly suffers at ranges beyond 40 m and drops to 0% detection rate at ranges beyond 100m. This shows the importance of retro-directivity in obtaining long range operation. Other factors affecting the operating range is the size of the Van Atta array as well as the the antenna gain at the tag. However, this defines a trade-off between the angular field of view and the covering range that needs to be considered based on the application needs.

Figures 14b and 14c show the median and 10^{th} and 90^{th} percentile errors of Millimetro as a function of distance from the radar. The figures demonstrate that Millimetro maintains the median range errors at 10-20 cm across different ranges up to 100m and azimuth estimates at 5-10 degrees. However, when moving to longer ranges, both the range and azimuth outlier errors increase, resulting in longer error bars. This is due to the SNR drops at longer ranges, which in turn drops the coding correlation for the tag detection.

7.3 Mobile Applications

Next, we evaluate Millimetro's performance in mobile scenarios, as a proof of concept for applications such as urban sensing, machine perception in robotics and autonomous driving. We conducted experiments in the open space, where the tag is placed at a fixed location and the radar is placed on a cart, bike, or car. For each of these setups, we perform 2-3 different experiments with different moving speeds

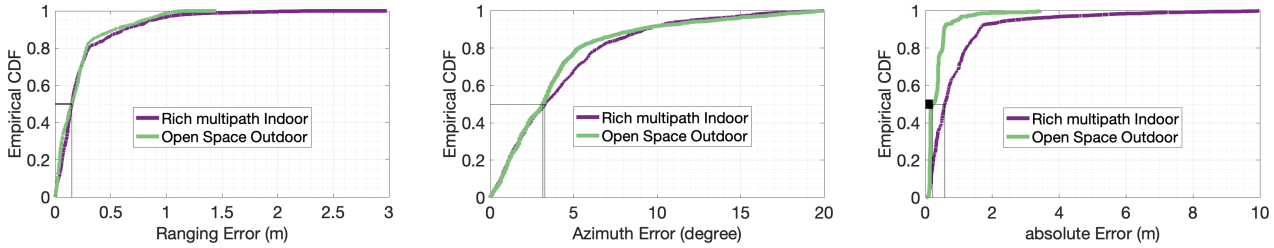

(a) Range Accuracy **(b) Azimuth Accuracy** **(c) 2D Localization Accuracy**

Figure 13: Localization performance.

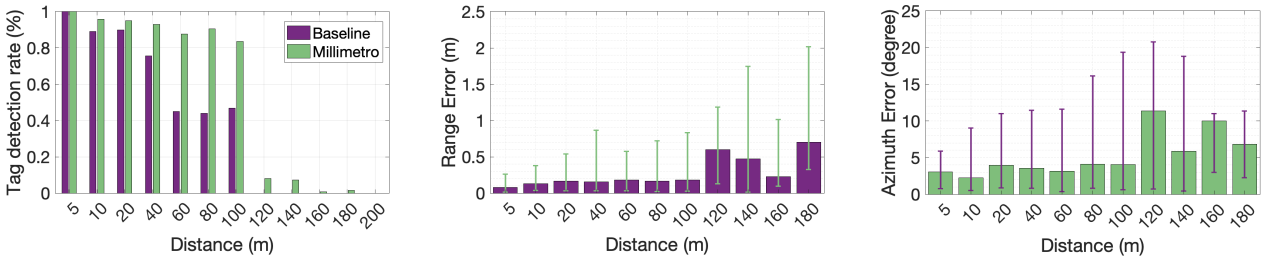

(a) Detection rate vs. Distance **(b) Range accuracy vs. Distance** **(c) Azimuth accuracy vs. Distance**

Figure 14: Performance as a function of distance.

Figure 15: Millimetro was tested in 3 mobile environments: walking, biking and driving.

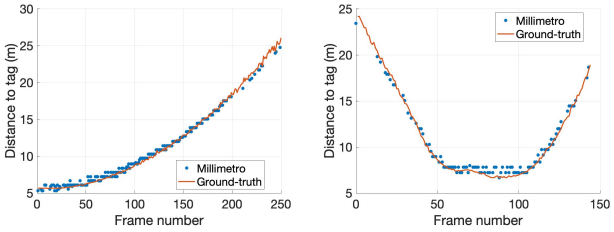

(a) Walking Snapshot **(b) Driving Snapshot**

Figure 16: Millimetro's ranging under mobility

(ranging from 3Km/h to 19Km/h) and different motion trajectories (i.e. approaching the tag or moving away from the tag). Snapshots of the setup is shown in Figure 15. To collect the ground truth, we used Aruco marker visual tracking system, which can cover ranges up to 30-40m. Therefore, the results provided in Figure 1 are only at locations that ground truths are available. We can see that the localization accuracy slightly degrades at higher speeds such as driving. Figures 16a and 16b also depicts snapshots of traces and range estimates for walking and driving experiments, with the ground truth up to the point it was detectable. We can see that Millimetro can maintain high ranging accuracy for extended distances even with mobility, making it a reliable sensing and localization mechanism for autonomous driving and robotic applications. In addition, with the small form-factor of mmWave radars and our retro-reflective tags, Millimetro can be easily used as a portable localization and sensing approach for many more applications such as industrial IoT and augmented reality, by embedding the tags in the environment or even the clothing of pedestrians.

7.4 Multi-Tag Performance

The Millimetro coding scheme combined with the asynchronous tag-reader framework allows a radar to localize multiple tags at the same time. We evaluate this by placing six different tags in a small indoor space and locating them from different ranges from the radar. The distance between tags changes from 50cm to 1.5m while the average distance of the radar to the tags varies between 3m to 15m, for a total of 50 experiments. During each experiment, all of the active tags constantly modulating, each at a certain frequency from the proposed coding scheme. For simplicity, we focus on range estimates and 1D localization. As shown in Figure 17a, the average ranging accuracy slightly decreases from 11 cm to 17 cm when 6 tags are active. We

	walk	bike	drive
median 1D Accuracy	20cm	30cm	31cm
90^{th} percentile (cm)	78cm	75cm	82cm

Table 1: Performance under mobility

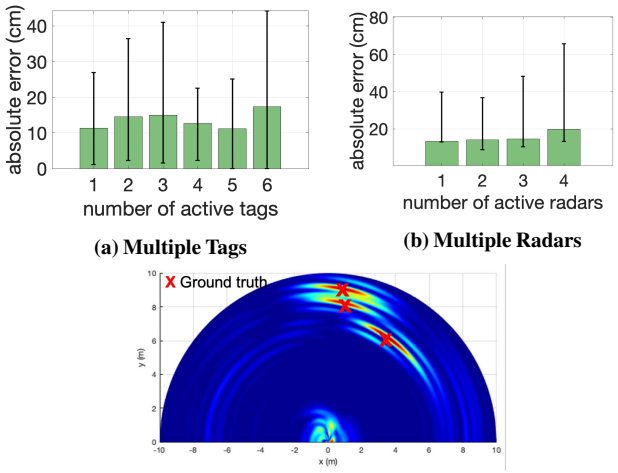

(a) Multiple Tags (b) Multiple Radars

(c) sample output with 3 active tags

Figure 17: Millimetro preserves the ranging performance under concurrent multi tag-reader operation.

realize that majority of errors happen for the tags that are co-located and having very similar modulation frequencies, resulting in confusion in the match filter correlations. This can be simply avoided at the time of tag deployment by selecting well-separated modulation frequencies for co-located tags.

7.5 Multi-Radar Performance

In addition to simultaneous reading of multiple tags, the Millimetro's tag retro-directivity as well as the adopted asynchronous tag-reader architecture enables concurrent multi-reader operation, where multiple radars can scan the same set of tags in their field of view at the same time. We evaluate the performance of Millimetro in this scenario by running over 20 experiments in different locations of the indoor office in ranges from 2 m to 17 m from the tag. We also varied the number of active radars from 1 to 4 without running any synchronization protocol between them. To stress test the system, two of the radars are always co-located and are only 20 cm apart on a table. We also repeated each experiment 5 times in each of which the radars are initiated in a random order. For the simplicity of ground-truth measurements, we focus on range estimates only. As shown in Figure 17b, the median range estimate errors increase from 10 cm in the presence of one active radar to 20 cm with 4 active radars. The main reason for performance degradation is the increase of multi-path interference between co-located radars. However, in real-world applications, there is typically a sufficient distance between radars to avoid such interference. Nevertheless, even with four concurrent active radars, Millimetro is capable of detecting and locating the tag.

7.6 Non-Line-of-Sight Performance

Next, we study Millimetro's tag localization performance in Non-Line-of-Sight (NLoS) scenarios. It is well-known that mmWave signals can be significantly attenuated by certain obstacles such as humans or a metal object, but we expect to detect the tag in several other kinds of obstructions that are common to robotic and autonomous driving scenarios such as having the tag in a box, behind a wall, or covered with snow or debris. We therefore evaluate the localization

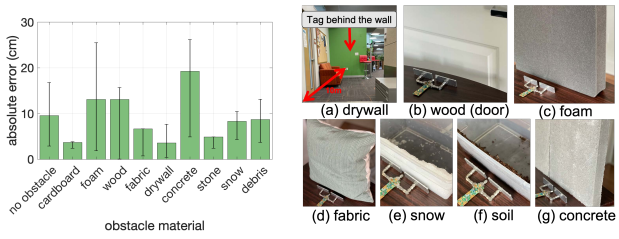

(a) (b)

Figure 18: Millimetro's (a) ranging accuracy when penetrating through (b) different materials/obstacles.

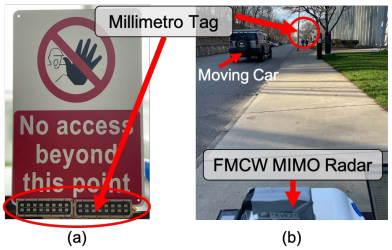

(a) (b)

Figure 19: Millimetro preserves high performance even when attached (a) on a metal surface or (b) at the presence moving cars.

performance of Millimetro while penetrating through different materials, as shown in Figure 18b. In our evaluation, we place the tag and radar at different ranges from 4 m to 20 m for a total of over 50 experiments. We then block the tag to radar view by placing large sheets of different materials with varying thicknesses and ensuring that line-of-sight view is completely obstructed. We also tested the penetration of the tag retro-reflection through one or multiple dry walls as well as snow and debris. Figure 18a demonstrates the median 1D localization errors across different materials. We can see that the ranging accuracy slightly decreases in the presence of an obstacle with a larger error for thicker and denser obstacles such as concrete or wood. However, the tag is still detectable even when going through multiple dry walls and at ranges above 15 m.

7.7 Multipath Effect

Finally, we evaluate the sensitivity of Millimetro to strong multipath signals such as the reflections from the road sign itself or varying multipath signals such as reflections from other moving cars on the road or people moving in the environment. We conduct several experiments to evaluate the multipath effect. First, we test the impact of strong reflections from nearby objects by placing the tag on a road sign (shown in Figure 19), near a car, or metal shelves in indoor environments. We notice no degradation in the tag localization performance. This is mainly because Millimetro looks for changes in the channel measurements in a frame to detect the tag. Therefore, it can easily resolve the dynamic range problem through background subtraction techniques by using the first chirp in a frame as the reference point.

Next, we perform an experiment with a fixed distance of 10 m between the tag and the reader and have 1 or 2 people moving in and around the line-of-sight between the tag and the reader. We performed a total of 5 experiments, in each case collecting over 300 frames. The five experiments include 1 or 2 person continuously crossing the LoS back and forth, 1 or 2 person walking on the sides of the LoS link, and

one person walking across the line in a zigzag motion. Across these experiments, we notice negligible impact on the Millimetro localization performance. This is mainly due to the way Millimetro detects the tag reflection by using the sinc template instead of solely relying on the modulation frequency. First of all the frequency range of Doppler shift and tag modulation are quite separated. In addition, even for very high speed moving cars in the environment, the tag modulation still carries a unique signature as a sinc function while the Doppler shift is a single frequency component. Millimetro uses this insight to differentiate the tag reflection from other varying multipath signals such as other moving cars in the environment. However in these experiments, the tag is missed a few times in the two person crossing experiments reducing the tag detection rate from 100% to 84%. This corresponds to the periods that all users are in the LoS completely blocking the tag to reader view. However, such missed detections can be easily handled by integrating measurements across multiple frames in more crowded areas.

8 RELATED WORK

Backscatter Localization: RFID is one of the first backscatter systems and different localization systems are built upon that by means of received signal strength [12], phase measurements [10, 31], or angle of arrival (AOA)-based triangulation [11, 54]. However, RFID protocol is limited to short ranges (<10m) and larger deployments and antenna arrays are required to achieve high accuracy. Recent work in this domain improves the localization accuracy of RFID systems by emulating larger bandwidths using frequency hopping or multi-frequency techniques [33, 35]. However, the higher accuracy is achieved at the expense of higher latency, hence disqualifying these methods as a portable localization solution.

Another line of research explores the use of UWB radios for backscatter localization [36, 37]. Despite several proposed techniques in the literature to combat the regulatory-constraints of UWB low transmission power, the short communication range is still one of the most limiting factors of this technology [15, 20, 37]. Some recent work addresses this issue by leveraging the entire ISM band below 10GHz to emulate a UWB channel [36]. However, the high range and accuracy in these solutions are achieved by complex reader setups and signal processing tricks, which make the system less robust specially in mobile and dynamic settings such as autonomous driving. WiFi backscattering has been also used for localization that leverages the ubiquity of WiFi infrastructure [29, 48], however such solutions are still limited to short ranges and indoor environments. Finally, plenty of work has been done on backscatter communication [17, 23, 52]. However, since these focus on communication, applying them to localization either compromises on power, range, or accuracy.

MMWave Backscattering: A few preliminary studies target the characterization of backscatter signals at mmWave frequency range [8, 19, 27, 28, 42], which are often compatible with the standard RFID architecture. Some other papers focus on energy harvesting [14, 21, 38] at short ranges or present new tag wake-up procedures [18]. Chipless mmWave RFID is another line of research that uses spatial-coded tags for identification [32, 40]. Even though these tags are completely battery-free, they are only detectable in short ranges (<1m). One of the main differences of Millimetro with these mmWave tags is the ultra low-power tag design as well as the asynchronous MAC protocol, which allows us to achieve long-range localization in practical scenarios such as automotive usecases.

Van Atta Tags: Different designs of planar Van Atta retro-reflectors are proposed for broad range of frequencies, some with pure passive configuration [9, 16, 22, 45], some with modulation capabilities [25, 30, 44, 51], and some with active components for enhancing the signal gain [26, 34, 46, 47]. The small form-factor of antennas in mmWave and THz bandwidths also attracted researchers to explore planer Van Atta structure in this frequency domain on flexible and rigid materials [24, 25, 43, 50, 51]. We adapt these techniques and build Millimetro on top of this research with a major focus on ultra-low-power modulation and the system stack for accurate long-range localization. In addition, we provide an extensive evaluation of such tags in practical scenarios by considering different factors such as long range, mobility, multipath, and obstacles.

9 CONCLUSION AND FUTURE WORK

This paper presents Millimetro, an ultra-low power tag for accurate localization at extended ranges. Millimetro achieves this through a novel mmWave retro-reflective tag that blends the localization accuracy at high-bandwidth mmWave frequencies with the extended range from a retro-directive tag design. We implement and evaluate our system indoors and outdoors demonstrating $< 3uW$ power requirements, centimeter-scale accuracy and extended (up to 100 meters) range. Millimetro is a natural solution for localizing roadside infrastructure for autonomous driving amidst poor weather or debris. Nevertheless, Millimetro still has some limitations including significant performance drop in complete NLoS scenarios and so machine perception in complete LoS blockage is still an open problem both in RF and vision-based systems (camera, LIDAR). In addition, Millimetro is currently evaluated in 24GHz instead of 77GHz, the main frequency band for automotive industry due to lack of RF components in higher frequency ranges. While such components may be increasingly available in the future this paper demonstrates a proof of concept design in the lower mmWave frequency range. It should be noted that all the techniques proposed in this paper can be seamlessly extended and implemented for higher frequencies.

Beyond autonomous driving, we believe Millimetro applies to industrial IoT, robotic systems and structural health monitoring. However, while our current evaluation is in 2D space, for such applications 3D localization is desirable, which can be easily achieved by leveraging a 2D MIMO radar (i.e. TIDEP-01012) to estimate elevation the same way we did for azimuth. We further note that to improve accuracy for these applications, Millimetro can leverage 77 GHz automotive radars that benefit from greater bandwidth, with our choice of 24 GHz radar for this work, dictated primarily by the availability of low-power components for tag hardware. We leave a rigorous evaluation of Millimetro's wide-ranging applications to future work. In addition, for Millimetro to be truly adopted at scale by the automotive industry, we will need to address security vulnerabilities like spoofing, which is part of our future work.

ACKNOWLEDGMENTS

This research was funded in part by the CONIX Research Center, one of six centers in JUMP, a Semiconductor Research Corporation (SRC) program sponsored by DARPA, and the National Science Foundation

(1718435, 1823235, 2030154 and 2007786). We thank our reviewers and shepherd for their insightful feedback which helped improve this paper. We also thank Prof. Mark Rodwell and his research group at the University of California Santa Barbara for their inputs.

REFERENCES

[1] Analong Devices SPDT Switch. https://www.analog.com/media/en/technical-documentation/data-sheets/ADRF5027.pdf, 2020.

[2] Analong Devices TinyRad. https://www.analog.com/media/en/technical-documentation/user-guides/ev-tinyrad24g-ug-1709.pdf, 2020.

[3] Energizer: Lithium Coin Handbook and Application Manual. https://data.energizer.com/pdfs/lithiumcoin_appman.pdf, 2020.

[4] Lunar Laser Ranging RetroReflector. https://www.nasa.gov/mission_pages/LRO/multimedia/lroimages/lroc-20100413-apollo15-LRRR.html, 2020.

[5] MACOM SPDT Switch. https://cdn.macom.com/datasheets/MASW_011102.pdf, 2020.

[6] P-SERIES NANOTRITIUM BETAVOLTAICS. https://citylabs.net/products/, 2020.

[7] Texas Instruments MSP430FR5994 microcontroller. https://www.ti.com/product/MSP430FR5994, 2020.

[8] A. O. Adeyeye, J. Hester, and M. M. Tentzeris. Miniaturized millimeter wave rfid tag for spatial identification and localization in internet of things applications. In *2019 49th European Microwave Conference (EuMC)*, pages 105–108. IEEE, 2019.

[9] A. A. Ali, H. B. El-Shaarawy, and H. Aubert. Millimeter-wave substrate integrated waveguide passive van atta reflector array. *IEEE transactions on antennas and propagation*, 61(3):1465–1470, 2012.

[10] D. Arnitz, K. Witrisal, and U. Muehlmann. Multifrequency continuous-wave radar approach to ranging in passive uhf rfid. *IEEE transactions on microwave theory and techniques*, 57(5):1398–1405, 2009.

[11] S. Azzouzi, M. Cremer, U. Dettmar, R. Kronberger, and T. Knie. New measurement results for the localization of uhf rfid transponders using an angle of arrival (aoa) approach. In *2011 IEEE International Conference on RFID*, pages 91–97. IEEE, 2011.

[12] M. Bouet and A. L. Dos Santos. Rfid tags: Positioning principles and localization techniques. In *2008 1st IFIP Wireless Days*, pages 1–5. Ieee, 2008.

[13] K. Chang and J. Wiley. *Encyclopedia of RF and microwave engineering*. Wiley-Interscience, 2005.

[14] M. S. Dadash, J. Hasch, and S. P. Voinigescu. A 77-ghz active millimeter-wave reflector for fmcw radar. In *2017 IEEE Radio Frequency Integrated Circuits Symposium (RFIC)*, pages 312–315. IEEE, 2017.

[15] N. Decarli, F. Guidi, and D. Dardari. Passive uwb rfid for tag localization: Architectures and design. *IEEE Sensors Journal*, 16(5):1385–1397, 2015.

[16] D. Desai, I. Gatley, C. Bolton, L. Rizzo, S. Gatley, and J. F. Federici. Terahertz van atta retroreflecting arrays. *Journal of Infrared, Millimeter, and Terahertz Waves*, 41(8):997–1008, 2020.

[17] A. Galisteo, A. Varshney, and D. Giustiniano. Two to tango: hybrid light and backscatter networks for next billion devices. 2020.

[18] F. Guidi, N. Decarli, D. Dardari, F. Mani, and R. d'Errico. Passive millimeter-wave rfid using backscattered signals. In *2016 IEEE Globecom Workshops (GC Wkshps)*, pages 1–6. IEEE, 2016.

[19] F. Guidi, N. Decarli, D. Dardari, F. Mani, and R. D'Errico. Millimeter-wave beamsteering for passive rfid tag localization. *IEEE Journal of Radio Frequency Identification*, 2(1):9–14, 2018.

[20] F. Guidi, A. Sibille, C. Roblin, V. Casadei, and D. Dardari. Analysis of uwb tag backscattering and its impact on the detection coverage. *IEEE transactions on antennas and propagation*, 62(8):4292–4303, 2014.

[21] A. Harutyunyan. Analog frontend for ultra low power 60-ghz rfid tag for back-scattering communication. In *Smart SysTech 2018; European Conference on Smart Objects, Systems and Technologies*, pages 1–7. VDE, 2018.

[22] D. Henry, J. G. Hester, H. Aubert, P. Pons, and M. M. Tentzeris. Long-range wireless interrogation of passive humidity sensors using van-atta cross-polarization effect and different beam scanning techniques. *IEEE Transactions on Microwave Theory and Techniques*, 65(12):5345–5354, 2017.

[23] M. Hessar, A. Najafi, and S. Gollakota. Netscatter: Enabling large-scale backscatter networks. In *16th {USENIX} Symposium on Networked Systems Design and Implementation ({NSDI} 19)*, pages 271–284, 2019.

[24] J. G. Hester and M. M. Tentzeris. Inkjet-printed flexible mm-wave van-atta reflectarrays: A solution for ultralong-range dense multitag and multisensing chipless rfid implementations for iot smart skins. *IEEE Transactions on Microwave Theory and Techniques*, 64(12):4763–4773, 2016.

[25] J. G. Hester and M. M. Tentzeris. A mm-wave ultra-long-range energy-autonomous printed rfid-enabled van-atta wireless sensor: At the crossroads of 5g and iot. In *2017 IEEE MTT-S International Microwave Symposium (IMS)*, pages 1557–1560. IEEE, 2017.

[26] T.-J. Hong, S.-J. Chung, et al. 24 ghz active retrodirective antenna array. *Electronics Letters*, 35(21):1785–1786, 1999.

[27] D. Hotte, R. Siragusa, Y. Duroc, and S. Tedjini. Radar cross-section measurement in millimetre-wave for passive millimetre-wave identification tags. *IET Microwaves, Antennas & Propagation*, 9(15):1733–1739, 2015.

[28] J. Kimionis, A. Georgiadis, and M. M. Tentzeris. Millimeter-wave backscatter: A quantum leap for gigabit communication, rf sensing, and wearables. In *2017 IEEE MTT-S International Microwave Symposium (IMS)*, pages 812–815. IEEE, 2017.

[29] M. Kotaru, P. Zhang, and S. Katti. Localizing low-power backscatter tags using commodity wifi. In *Proceedings of the 13th International Conference on emerging Networking EXperiments and Technologies*, pages 251–262, 2017.

[30] S. Kunpeng and F. Dejun. The frequency-shifting modulation of radar signal using active van atta array. In *2019 IEEE 4th International Conference on Signal and Image Processing (ICSIP)*, pages 509–512. IEEE, 2019.

[31] X. Li, Y. Zhang, and M. G. Amin. Multifrequency-based range estimation of rfid tags. In *2009 IEEE International Conference on RFID*, pages 147–154. IEEE, 2009.

[32] Z. Li, B. Chen, Z. Yang, H. Li, C. Xu, X. Chen, K. Wang, and W. Xu. Ferrotag: a paper-based mmwave-scannable tagging infrastructure. In *Proceedings of the 17th Conference on Embedded Networked Sensor Systems*, pages 324–337, 2019.

[33] Z. Luo, Q. Zhang, Y. Ma, M. Singh, and F. Adib. 3d backscatter localization for fine-grained robotics. In *16th {USENIX} Symposium on Networked Systems Design and Implementation ({NSDI} 19)*, pages 765–782, 2019.

[34] C. Luxey and J.-M. Laheurte. A retrodirective transponder with polarization duplexing for dedicated short-range communications. *IEEE transactions on microwave theory and techniques*, 47(9):1910–1915, 1999.

[35] Y. Ma, N. Selby, and F. Adib. Minding the billions: Ultra-wideband localization for deployed rfid tags. In *Proceedings of the 23rd Annual International Conference on Mobile Computing and Networking*, pages 248–260, 2017.

[36] R. Nandakumar, V. Iyer, and S. Gollakota. 3d localization for sub-centimeter sized devices. In *Proceedings of the 16th ACM Conference on Embedded Networked Sensor Systems*, pages 108–119, 2018.

[37] P. Pannuto, B. Kempke, and P. Dutta. Slocalization: Sub-uw ultra wideband backscatter localization. In *2018 17th ACM/IEEE International Conference on Information Processing in Sensor Networks (IPSN)*, pages 242–253. IEEE, 2018.

[38] S. Pellerano, J. Alvarado, and Y. Palaskas. A mm-wave power-harvesting rfid tag in 90 nm cmos. *IEEE Journal of Solid-State Circuits*, 45(8):1627–1637, 2010.

[39] C. Pon. Retrodirective array using the heterodyne technique. *IEEE Transactions on Antennas and Propagation*, 12(2):176–180, 1964.

[40] S. Preradovic and N. Karmakar. Chipless millimeter wave identification (mmid) tag at 30 ghz. In *2011 41st European Microwave Conference*, pages 123–126. IEEE, 2011.

[41] T. S. Rappaport, J. N. Murdock, and F. Gutierrez. State of the art in 60-ghz integrated circuits and systems for wireless communications. *Proceedings of the IEEE*, 99(8):1390–1436, 2011.

[42] W. Scheiblhofer, R. Feger, A. Haderer, S. Scheiblhofer, and A. Stelzer. Simultaneous localization and data-interrogation using a 24-ghz modulated-reflector fmcw radar system. In *2017 IEEE MTT-S International Microwave Symposium (IMS)*, pages 67–70. IEEE, 2017.

[43] C. M. Schmid, R. Feger, and A. Stelzer. Millimeter-wave phase-modulated backscatter transponder for fmcw radar applications. In *2011 IEEE MTT-S International Microwave Symposium*, pages 1–4. IEEE, 2011.

[44] K. Song, D. Feng, J. Wang, Q. Xie, and L. Liu. Phase modulation of retro-reflected radar echo signal using a microstrip van-atta array. *IEEE Access*, 7:96011–96018, 2019.

[45] R. Sorrentino, E. Sbarra, L. Urbani, S. Montori, R. V. Gatti, and L. Marcaccioli. Accurate fmcw radar-based indoor localization system. In *2012 IEEE International Conference on RFID-Technologies and Applications (RFID-TA)*, pages 362–368. IEEE, 2012.

[46] A. Strobel, C. Carlowitz, R. Wolf, F. Ellinger, and M. Vossiek. A millimeter-wave low-power active backscatter tag for fmcw radar systems. *IEEE transactions on microwave theory and techniques*, 61(5):1964–1972, 2013.

[47] J. Thornton and D. Edwards. Range measurement using modulated retro-reflectors in fm radar system. *IEEE microwave and guided wave letters*, 10(9):380–382, 2000.

[48] X. Tong, F. Zhu, Y. Wan, X. Tian, and X. Wang. Batch localization based on ofdma backscatter. *Proceedings of the ACM on Interactive, Mobile, Wearable and Ubiquitous Technologies*, 3(1):1–25, 2019.

[49] L. C. Van Atta. Electromagnetic reflector, Oct. 6 1959. US Patent 2,908,002.

[50] J. A. Vitaz, A. M. Buerkle, M. Sallin, and K. Sarabandi. Enhanced detection of on-metal retro-reflective tags in cluttered environments using a polarimetric technique. *IEEE transactions on antennas and propagation*, 60(8):3727–3735, 2012.

[51] J. A. Vitaz, A. M. Buerkle, and K. Sarabandi. Tracking of metallic objects using a retro-reflective array at 26 ghz. *IEEE transactions on antennas and propagation*, 58(11):3539–3544, 2010.

[52] P. Wang, L. Feng, G. Chen, C. Xu, Y. Wu, K. Xu, G. Shen, K. Du, G. Huang, and X. Liu. Renovating road signs for infrastructure-to-vehicle networking: a visible light backscatter communication and networking approach. In *Proceedings of the 26th Annual International Conference on Mobile Computing and Networking*, pages 1–13, 2020.

[53] S. Xu, B. J. Kooij, and A. Yarovoy. Joint doppler and doa estimation using (ultra-) wideband fmcw signals. *Signal Processing*, 168:107259, 2020.

[54] J. Zhou, H. Zhang, and L. Mo. Two-dimension localization of passive rfid tags using aoa estimation. In *2011 IEEE International Instrumentation and Measurement Technology Conference*, pages 1–5. IEEE, 2011.